Solid State Ionics 357 (2020) 115463

Contents lists available at ScienceDirect

Solid State Ionics

journal homepage: www.elsevier.com/locate/ssi

Computational investigation of silicene/nickel anode for lithium-ion battery

Alexander Y. Galashev[a,b,*]

[a] Institute of High-Temperature Electrochemistry, Ural Branch, Russian Academy of Sciences, Sofia Kovalevskaya Str. 22, Yekaterinburg 620990, Russia
[b] Ural Federal University named after the first President of Russia B.N. Yeltsin, Mira Str., 19, Yekaterinburg 620002, Russia

ARTICLE INFO

Keywords:
Defects
Lithium ion
Molecular dynamics
Nickel
Silicene
Stress

ABSTRACT

Silicon-based anodes are distinguished by an exceptionally high energy capacity, which is an order of magnitude superior to that of a graphite anode. The thin-film design of the anode creates the conditions for increasing the specific energy, energy density and power density of LIB. Bilayer silicene on a nickel substrate is the anode material that can increase LIB performance. In the present work, using the molecular dynamic method, a detailed analysis of the packings of lithium atoms in silicene channels with different types of walls is performed. The occupancy of the channels with lithium depends on the type of defects present in its walls. Lithiation and delithiation are carried out in the presence of a constant electric field. The type of substrate affects the packing of lithium atoms in the channel and consequently on battery capacity and performance. The maximum filling of the lithium channel is achieved when monovacancies are present in silicene sheets. It is shown that the most preferable location of Li atoms in a channel is their location over hexagonal Si cells. The most significant stresses in silicene σ_{zz} are maximal in the presence of trivacancies in silicene sheets.

1. Introduction

The development of stable anode materials, providing a high energy and power density during long-term cycling is a priority when creating lithium-ion batteries (LIBs) of a new generation [1]. When improving LIBs, complex synthesis procedures and the use of expensive materials should be excluded [2]. In general, the use of silicon materials, meets this requirement. In particular, the relative cheapness of silicon is due to its wide distribution in the Earth's crust, as well as the ability of silicon atom to bind to four lithium atoms, which makes it possible to achieve an extremely high electrode capacity.

Silicon has a high theoretical gravimetric capacity (~4200 mA h g^{-1}), which is significantly higher than the capacity of graphite (372 mA h g^{-1}) [3,4]. Although bulk silicon has a very high capacity, it experiences a rapid degradation with each cycle due to a substantial increase in the electrode volume (up to 300%) during lithiation [2]. Such an electrode swelling creates a large load on the material [5,6]. Unlike graphite, lithium is introduced into silicon in the form of neutral atoms, not ions [5].

Fundamental research aimed at finding reliable, high-performance Si anodes allows a detailed study of the lithization mechanism, knowledge of which is important for the construction of Si anodes. A number of works are devoted to the study of changes in the mechanical properties during lithiation of silicon [7–10] and silicene [11–13].

Silicene can be considered as a silicon analog of graphene. However, there are some fundamental differences in the structure of these two-dimensional materials. Unlike graphene, the Si atoms in silicene are not in the same plane. If graphene can be obtained from graphite by exfoliating its layers, then such a possibility is not foreseen for obtaining silicene, because there is no natural silicon multilayer material like graphite. The two-dimensional form of silicon is prone to bending, more specifically buckles. The silicene structure is formed not only on the basis of sp^2 hybridization, but also with some participation of sp^3 hybridization. The epitaxially grown silicene sheets are not detached from the substrate.

Silicene having an atomic thickness can serve as a high-capacity host of Li in lithium-ion rechargeable batteries [14,15]. During the adsorption of alkali metals with silicene, a significant charge transfer occurs from the metals Li, Na, and K to two-dimensional silicon, as a result of which the metallization of silicene occurs [16]. The maximum energy barrier for the migration of Li/Li^+ adatoms along the sides of a silicene is only 1.70/1.75 eV [17]. A low-energy barrier means that Li adatoms can easily penetrate into two-layer or multi-layer silicone [18]. Greater charge storage capacity and better energy density of silicene compared with graphene are the basis for improving the performance of LIBs.

* Corresponding author at: Institute of High-Temperature Electrochemistry, Ural Branch, Russian Academy of Sciences, Sofia Kovalevskaya Str. 22, Yekaterinburg 620990, Russia
E-mail address: galashev@ihte.uran.ru.

https://doi.org/10.1016/j.ssi.2020.115463
Received 29 April 2020; Received in revised form 21 July 2020; Accepted 7 September 2020
Available online 13 October 2020
0167-2738/

The presence of defects has a great effect on mechanical, thermodynamic and electronic properties of two-dimensional materials. Conducted experiments have provided clear evidence of the presence of larger multivacancies in silicene [19,20]. The structure of the main defects, their stability, and mechanism of formation to a certain extent, they were considered in [19]. Sometimes small defects are introduced purposefully for specific applications [20]. In particular, it is known that the creation and elimination of point defects provides a simple way for the targeted adjustment of the local structure, thermal stability and the band gap of low-dimensional materials [21].

The proposal to use Ni as an inactive material in the construction of the LIB anode was made in [22]. This is due to the fact that Ni has a high electrical conductivity, low cost and good adhesion to Si. It is extremely important to take into account the influence of the substrate on the functioning of 2D materials in the LIB. The work [23] emphasizes the significant influence of "inert" materials included in the construction of a thin-film silicon anode on the functioning of this electrode. Based on computer simulation [24–26], we investigated the ability of a pair of "two-layer silicene on an Ag(111) substrate" to be represented as an anode material of a lithium-ion battery (LIB). It has been shown that this pair is not the best option when using silicene for this purpose [26]. It turns out that a nickel substrate can constitute a worthy competition for a silver substrate in an electrochemical device.

The capacity of the film electrode on the nickel substrate will depend on how the Li atoms are packed in a silicene channel. Since the channel is rather narrow, the boundary conditions, i.e. the channel walls will affect the nature of the packing of lithium atoms in it. We used the channel walls formed by both perfect and defective silicene. Defects were formed by removing one, two, three, and six compactly positioned Si atoms. In certain cases, the capacity of the electrode can be increased due to the high concentration of defects [11–15]. A more detailed study of the processes occurring in the LIB can be performed using computer simulation.

The purpose of this work is to study the effect of the Ni(111) substrate on the physical properties of the silicene channel supported by it, as well as on the determination of the effect of the type of vacancy defects in silicene on the completeness of filling the channel with lithium and on the stresses generated in it.

2. Materials and methods

Silicene is almost impossible to separate from the metal substrate on which it is obtained. Therefore, it is on this substrate that silicene is supposed to be used as the anode material. In this case, the silicene should have a fairly good electrical contact with an external electrical circuit, and the substrate should not have contact with the cathode.

Investigations on the development of technology for producing high-quality thin-film anodes are of considerable interest for the development of flexible electronics. The use of thin-film electrodes does not guarantee that all problems associated with premature LIB degradation will be solved. For example, problems associated with the appearance of cracks and peeling of the film from the substrate may arise here [27].

The present study is based on the results of the classical molecular dynamic (MD) calculations performed by us. We use Tersoff potential to describe Si–Si interactions within each sheet of silicene. The parameters of this potential are given in [28]. The Ni–Ni interaction was considered in the model using modified potential of an embedded atom [29]. The remaining interatomic interactions (Si–Si for different sheets of silicene, Li–Li, Li–Si, Li–Ni, and Si–Ni) in the system were described by the Morse potential with parameters taken from (see Table 1) [30–33].

2.1. Model

The unit cell of perfect silicene consisted of 18 Si atoms (Fig. 1), six of which were above the main plane (in which 12 other atoms are located) at a distance of 0.074 nm. Such a structure was obtained in a physical experiment on an Ag(111) substrate [32]. It was identified using non-contact atomic force microscopy, scanning tunneling microscopy, angle-resolved photoelectron spectroscopy, and low-energy electron diffraction [34]. It was shown that a monolayer of epitaxial silicene with such a structure occupies most of the surface on an Ag (111) substrate [35].

Table 1
Parameters of Morse potential describing various interactions.

Interaction[a]	D_0 (meV)	α (nm^{-1})	r_m (nm)
$Si^{(1)}$–$Si^{(2)}$	227.40	44.992	0.154
Li–Li	420.76	7.899	0.300
Li–Si	309.30	36.739	0.116
Li–Ni	420.63	11.049	0.288
Ni–Si	309.20	14.794	0.353

[a] The upper indices at Si denote the belonging to the layer of atoms 1 or 2.

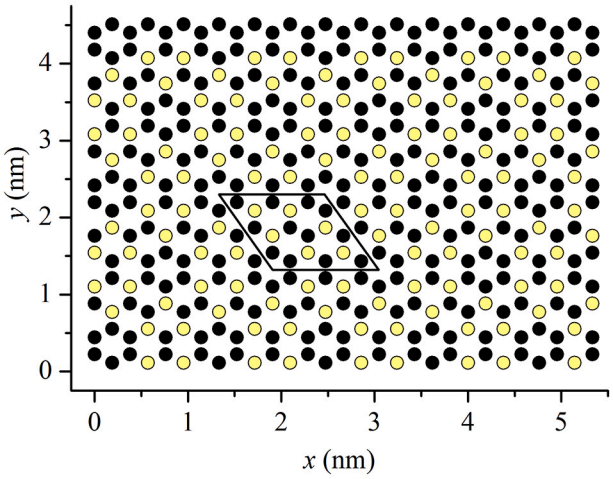

Fig. 1. Top view of the silicene structure at the initial instant; light colored circles are Si atoms displaced normally to the surface, dark circles are Si atoms in the initial plane; an outline shows a unit surface cell of the silicene sheet.

Point defects in the form of mono- and bi-vacancies, as a rule, are always present in silicene produced on metal surfaces. So, on the substrate Ag(111), the concentration of mono- and bivacancies reaches 4.4×10^{13} and 5.0×10^{13} cm^{-2}, respectively [36]. At this concentration, one defect will be contained in each area of 2 nm^2. The low stability of silicene is partly due to the high concentration of point defects, their easy diffusion and tendency to coalescence.

In the calculations performed, the size of the silicene sheet was 4.8×4.1 nm (taking into account the size of Si atoms), and the width of the gap between the silicene sheets was $h_g = 0.75$ nm. Previously, we established that, with this gap size, one Li^+ ion could move in a silicene channel, without leaving it, for 100 ps, when the electric field strength was 10^3 V/m [37]. Almost the same electric field (when creating a working voltage of 1.5 V) is achieved in LIB, when a LiPON film ~30 μm thick is used as a solid electrolyte [38]. The perfect silicene sheet contained 300 atoms. We also performed calculations for channels whose walls are not formed by an ideal silicene. In this case, 9 vacancy defects were formed in each sheet of silicene. Four types of defects were considered: mono-, bi-, tri-, and hexa-vacancies. Nine identical defects were placed approximately evenly with a shift of 0.1–0.2 nm in each (x and y) direction for different silicene sheets. Silicene sheet containing mono-, bi-, tri- and hexa-vacancies was formed from 291, 282, 273, and 246 Si atoms, respectively. The stacking of Bernal (ABAB …) was exactly the same as for the graphene sheets in graphite, which was carried out while creating flat, perfect and defective silicene channels [39]. The equations of motion were

solved by the Runge-Kutta method of order 4 with a time step $\Delta t = 1 \times 10^{-16}$ s.

2.2. The processes of lithiation and delithiation

Li^+ ions were introduced into the silicene channel and were removed from it in pairs under the influence of a constant electric field. The Li atom has a very low diffusion barrier in a thin layer of amorphous silicon (~0.5 eV) [40]. The interaction of silicene with the substrate and with Li atoms adsorbed and the presence of vacancy defects in silicene can change the silicene buckle height Δh and the Si—Si bond length L_{av}. We observed changes in buckle height and bond lengths in the ranges of $0.06 \le \Delta h \le 0.12$ nm and $0.231 \le L_{av} \le 0.243$ nm, respectively. The average Si—Li bond length obtained was 0.265 nm, which is in good agreement with the data of [41]. The adsorption energy values determined for lithium by us on silicene were from 2.27 to 2.52 eV/Li (depending on the location of the Li atom).

The pairwise introduction of ions into the channel, as well as their pairwise removal from the channel, accelerates the modeling process twice, however, the main goal of the chosen modeling method was to show that taking into account the Coulomb interaction between two ions does not distort the processes of filling the channel with lithium and freeing it from lithium. We performed a similar simulation when the processes of filling and emptying the channel with lithium were performed in the presence of only one charged atom (while other atoms had no charge) in the channel, including this was also done for other systems [14,15]. We did not observe a numerical difference in the maximum filling of the channel with lithium performed by these methods. However, the exit of ions from the channel in the case of the presence of the Coulomb interaction between the ions making up the pair occurred somewhat faster than in the case when there was no such interaction (since only one ion was present in the channel).

The ion introduced into the channel remains in it for 10 ps. This is mainly due to the fact that the ion cannot overcome the barrier created by the attracting interaction of other atoms. When a lithium ion is converted to a Li atom (after a set time of 10 ps), the nature of its interaction with other atoms (Si and Li) did not change, but the electric field no longer had any influence on it. In other words, the transition of the Li^+ ion to an atom meant a change in its electric charge from $+1e$ to 0 (every 10 ps), which did not affect its interactions not related to the presence of an electric charge. After every 10 ps, a new Li^+ ion was launched into the channel. This procedure was repeated until the ions could find a place in the channel. The limiting number of introduced lithium atoms turned out to be 74 in the case of a channel from a perfect silicene. All attempts to increase the number of Li atoms above this value were unsuccessful, since the Li^+ ion eventually either left the channel outward, or did not enter in the channel at all. At the end of filling the channel with lithium, we obtained a system in which electrically charged particles (ions) are completely absent.

During the process of delithiation, the charged particle was again present in the system. The process of delithiation was carried out when the direction of the electric field was reversed and the modulus of this magnitude was increased to 10^5 V/m. The order of appearance of the ion in the system also had an inverse order, i.e. the last of Li^+ ions that got into the channel became the first one, etc. The lifetime of the ion remained the same, i.e. was 10 ps. Ion always left the channel during its lifetime and left the channel without the accompaniment of lithium atoms. It was established in a separate series of calculations that such a character of the inverse process is not related to the order in the sequence of conversion of atoms into ions. It was shown that a change in the order of the exit of ions from the channel did not lead to any new result. So that, when the choice of the outgoing ions was made randomly, each ion came out from the channel alone without the accompaniment of other atoms.

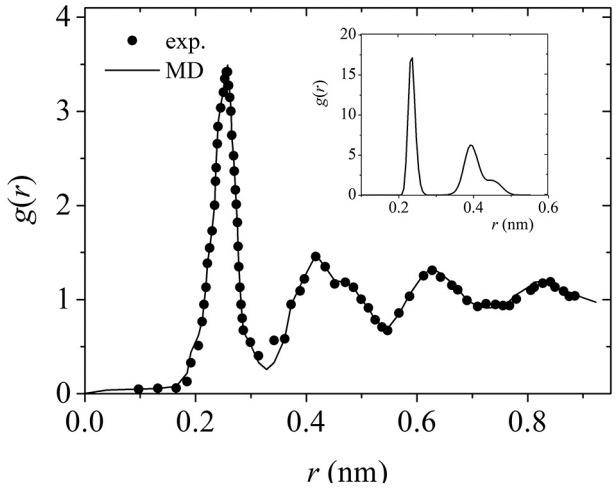

Fig. 2. The radial distribution function of a nickel and silicene (in insert) crystal at 300 K. The inset shows the $g(r)$ function obtained in the MD calculation for freestanding silicene at the same temperature.

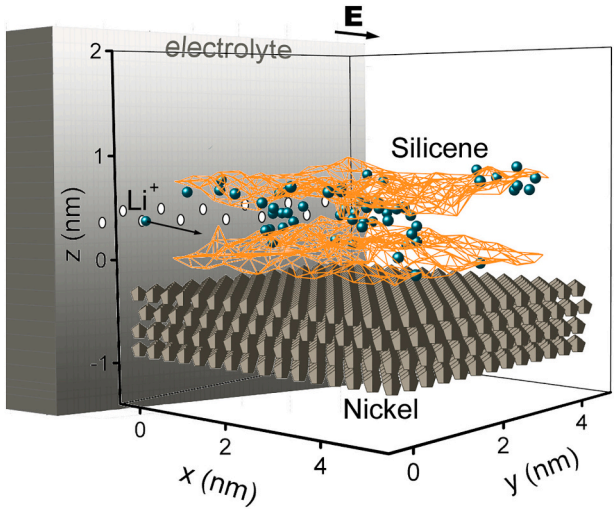

Fig. 3. The channel, formed by perfect silicene sheets, on the substrate Ni(111) after 500 ps of the lithium filling process.

2.3. Determination of stresses and structural properties

Our method for calculating the stress distribution in silicene sheets is as follows. We divide the sheets of silicene into elementary areas with the normal γ (x, y, z) and elongated either in the “armchair” direction or in the “zigzag” direction. Next, the resulting force acting on each of the areas is determined. In determining the resultant force, only those interactions between particles i and j are taken into account, the force vector of which pierces the given area [42]. In addition, the calculation of $\sigma_{\gamma\alpha}(l)$ takes into account the directions α (x, y, z) of the velocities of the atoms i and j [43]:

$$\sigma_{\gamma\alpha}(l) = \left\langle \sum_i^n \frac{1}{\Omega}(m v_\gamma^i v_\alpha^i) \right\rangle + \frac{1}{S_l} \left\langle \sum_i^n \sum_{j \ne i}^{(u_i \le u u_j \ge u)} (f_{ij}^\alpha) \right\rangle \quad (1)$$

In expression (1), the following notation is used: n is the number of atoms on the lth area, Ω is the volume per atom, m is the atomic mass, $v_\alpha{}^i$ is the α projection of the velocity of the ith atom, S_l is the area of the lth surface element, $f_{ij}{}^\alpha$ is the α projection of the force resulting from the interaction of i and j atoms and passes though the lth area, and u_i is the coordinate of the atom i; the symbol u denotes the coordinate of the contact point of the straight line through the centers of the atoms i and j

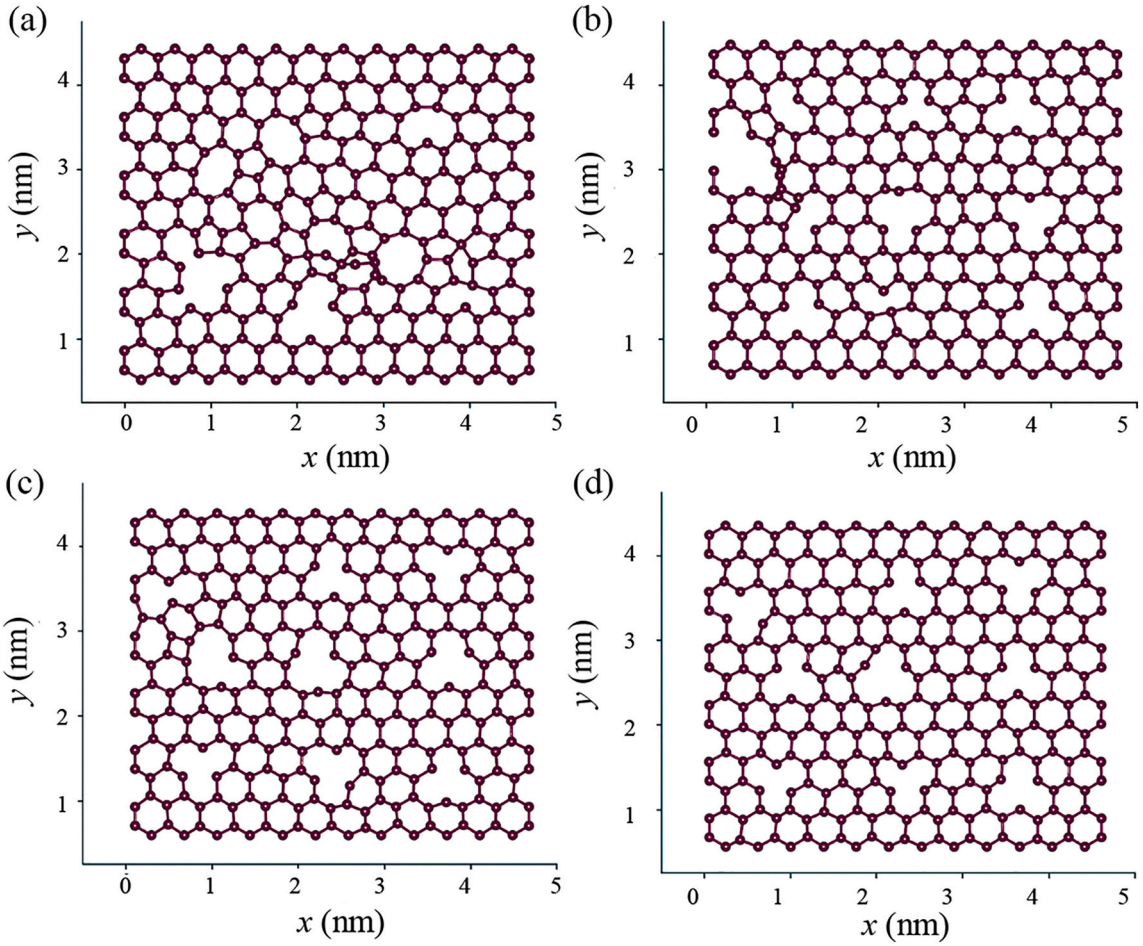

Fig. 4. x–y Projections of the top sheet of silicene with mono vacancies, on metal substrates: (a) Ag, (b) Al, (c) Cu, (d) Ni after the end of the lithiation/delithiation cycle.

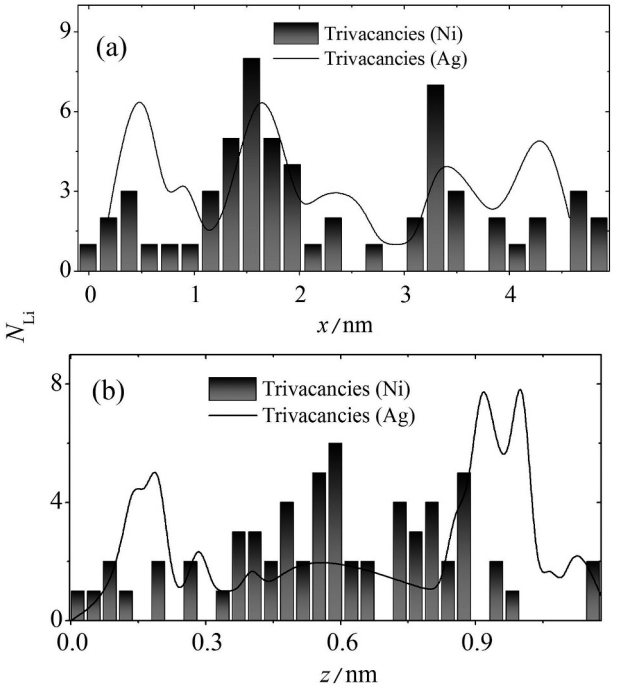

Fig. 5. (a) Horizontal (longitudinal) and (b) vertical profiles of lithium density in a silicene channel with trivacancies on Ni(111) and Ag(111) substrates.

and the *l*th surface element.

The method of statistical geometry is a powerful tool in the structural analysis of mainly irregular packing of various entities, including those located in a limited space. This method consists in dividing the three-dimensional space between entities. Each entity is assigned a certain portion of the space in the shape of a polyhedron. In the original version, the partition of space corresponded to the construction of Voronoi polyhedra (VP) [44,45]. When constructing VPs for the packaging of lithium atoms contained in a silicene channel, one can include in considering the influence of the channel walls on the local environment of the atoms. The influence of the channel walls is taken into account by comparing the statistical distributions of elements of polyhedra whose faces are solely due to the presence of Li atoms, with the corresponding distributions of polyhedra with faces originating from Li and Si neighbors. Polyhedrons formed together by Li and Si neighbors surrounding the Li atom will be called combined polyhedra (CP). Thus, cyclic structures of Li atoms form the faces of VPs and the corresponding structures of Li and Si atoms create faces of CPs. The difference in the sizes of the Li and Si atoms in the construction of the CP is not taken into account. Small geometric elements in Voronoi polyhedra, created by thermal fluctuations, make it difficult to carry out reliable structural analysis. Elimination of small edges and faces of VP can be performed by going into the analysis of simplified polyhedra (SP) [46]. As in the case with VP, we will consider both SP and the corresponding combined polyhedra (CSP) corresponding to them, constructed taking into account both Li and Si potential neighbors. A more complete description of the models used is given in Supporting Information.

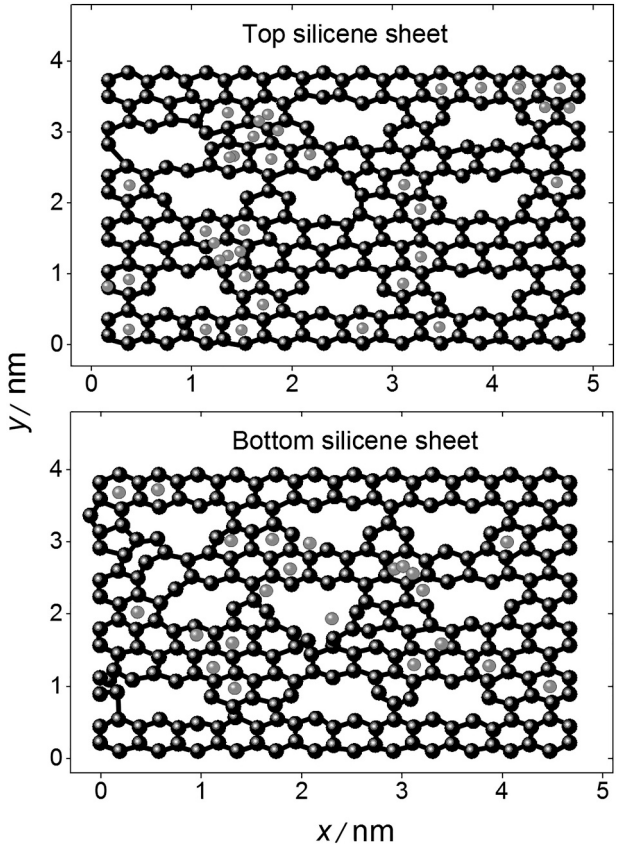

Fig. 6. x–y-Projections of the upper and lower sheets of silicene with trivacancies on the Ni(111) substrate, at the time of complete lithiation (60 lithium atom was adsorbed on the silicene surface). Si atoms form a network.

To perform parallel computations, we used the LAMMPS code intended for molecular dynamic simulation [47]. We made the LAMMPS extension by introducing our own fragment to calculate the mechanical properties of the system. These calculations were performed on a hybrid cluster calculator "Uran" at IMM UB RAS with a peak performance of 216 Tflop s^{-1} and 1864 CPU.

3. Results and discussion

3.1. Model validation and simulation design

To test the selected interatomic potentials, using the 32000 atom MD model of nickel crystal and the 9600 atom MD model of freestanding silicene, we calculated the radial distribution functions $g(r)$ of these objects. Fig. 2 shows a comparison of the function $g(r)$ calculated by us for the Ni crystal at $T = 300$ K with the corresponding function obtained experimentally [48]. The inset of this figure shows the function $g(r)$ calculated by us for freestanding silicene at the same temperature. The shape of this function exactly coincides with $g(r)$ obtained in the MD calculation under identical conditions and with the same number of atoms [49]. The results of the performed verification give reason to believe that the model we are using is adequate.

The configuration of the "Ni–Si–Li" system, referring to a time point of 500 ps at the filling by lithium of the channel formed by sheets of perfect silicene, is shown in Fig. 3. During this time, 50 lithium ions were introduced into the channel. All Li atoms in the channel are visible in the figure, because silicene sheets are shown as transparent. A significant part of Li atoms is located on the outer surface of strongly deformed silicone sheets. They can get there through the gap between the impermeable side walls (not shown in the Fig. 3) and the edges of the sheets. It is obvious that the majority of Li atoms belong to the upper sheet. There are no Li atoms that were significantly removed from the "silicene channel on the Ni(111) substrate" system. This is the result of the influence of the metal substrate, since in the absence of a substrate the number of adsorbed Li atoms by each silicene sheet is approximately equal.

Previously, we performed similar studies of the applicability of silicene on other metal substrates (Ag, Al, Cu) as an anode material [11–13]. The effect of the substrate on silicene is shown in Fig. 4, which shows the x–y projections of the upper sheets of a two-layer silicene located on metal substrates after a complete lithiation/delithiation cycle. As can be seen from the Fig. 4, the shape of defects (monovacancies) is best preserved when silicene is on the Ni(111) substrate. The use of this substrate also achieves the greatest filling of the silicene channel with lithium during lithiation. On the Ag(111) substrate, the shape of vacancies after the completion of the cycle becomes predominantly rounded; on the Al(111) substrate, some monovacancies shrink or, conversely, expand; the same, albeit to a lesser extent, is observed in the case of using a Cu(111) substrate.

3.2. Channel filling with lithium

The limiting filling of the channel with lithium led to the highest height of the dome formed by the lower sheet of silicene. The highest domes were formed for sheets of perfect silicene and silicene with hexavacancies. The deformation of silicene sheets leads to a decrease for space available for filling the channel with lithium, which in the case of perfect silicene reached 22%. Strong deformations of silicene sheets on the Ni(111) substrate contribute to the structural rearrangement of vacancy-type defects in silicene. The magnitude of the vertical deformation for sheets of silicene with defects as well as the volume change of the inter-sheet space were not as strong as for perfect silicene. The exception was the channel with hexavacancies, where the reduction in the volume of the channel after filling it with lithium was ~25%. The horizontal (along the axis 0x) and the vertical (along the axis 0z) profiles of lithium density in the silicene channel are usually of the same type for both perfect silicene sheets and sheets with various vacancies-type defects. Fig. 5 shows the corresponding profiles of numerical density in the case of presence of trivacancies in silicene. The values of x and z are calculated from the entrance to the channel ($x = 0$) and from the level of the lower sheet of silicene ($z = 0$).

Because of the obstacles to moving which connect with the deformation of the channel on the Ni(111) substrate, the Li atoms fill the channel rather unevenly. As can be seen from Fig. 5a, the channel has a more intense fill density in the intervals $1 < x < 2$ and $3.0 < x < 3.6$. The channel on the Ag(111) substrate is also filled with lithium in the horizontal direction somewhat uneven, showing a larger population in the first half of the channel length (57.5%) and a smaller population in the second half of the channel length (42.5%) (Fig. 5a). The vertical profile shows a denser filling of the channel with lithium on the substrate Ni(111) in the middle part and a low content of Li atoms immediately near the walls. If a similar channel located on an Ag(111) substrate was filled with lithium, a different picture was observed. The channel remained half-empty at mid-height, i.e., Li atoms adjacent to the upper and lower sheets turned out to be separated. The results of MD simulations show that the shape of vacancy defects is not preserved when lithium fills the channel regardless of whether the channel is on the Ni(111) substrate or the Ag(111) one.

Let us consider in more detail behavior of the defects and attribution of the Li atoms to the silicene sheets by the example of a silicene channel having trivacancies and fully filled with lithium. The investigated configurations refer to the instant 0.60 ns (or 6.0×10^6 Δt). The xy projections of the upper and lower layers of the channel cut by the mean ($z = h_g^*/2$) plane are shown in Fig. 6. The view is given from the side of the plane $z = h_g^*/2$. Here, h_g^* is the vertical channel size after lithiation. xy projections show that after 100 ps, both the upper and the lower sheets of the silicene retained the original number of

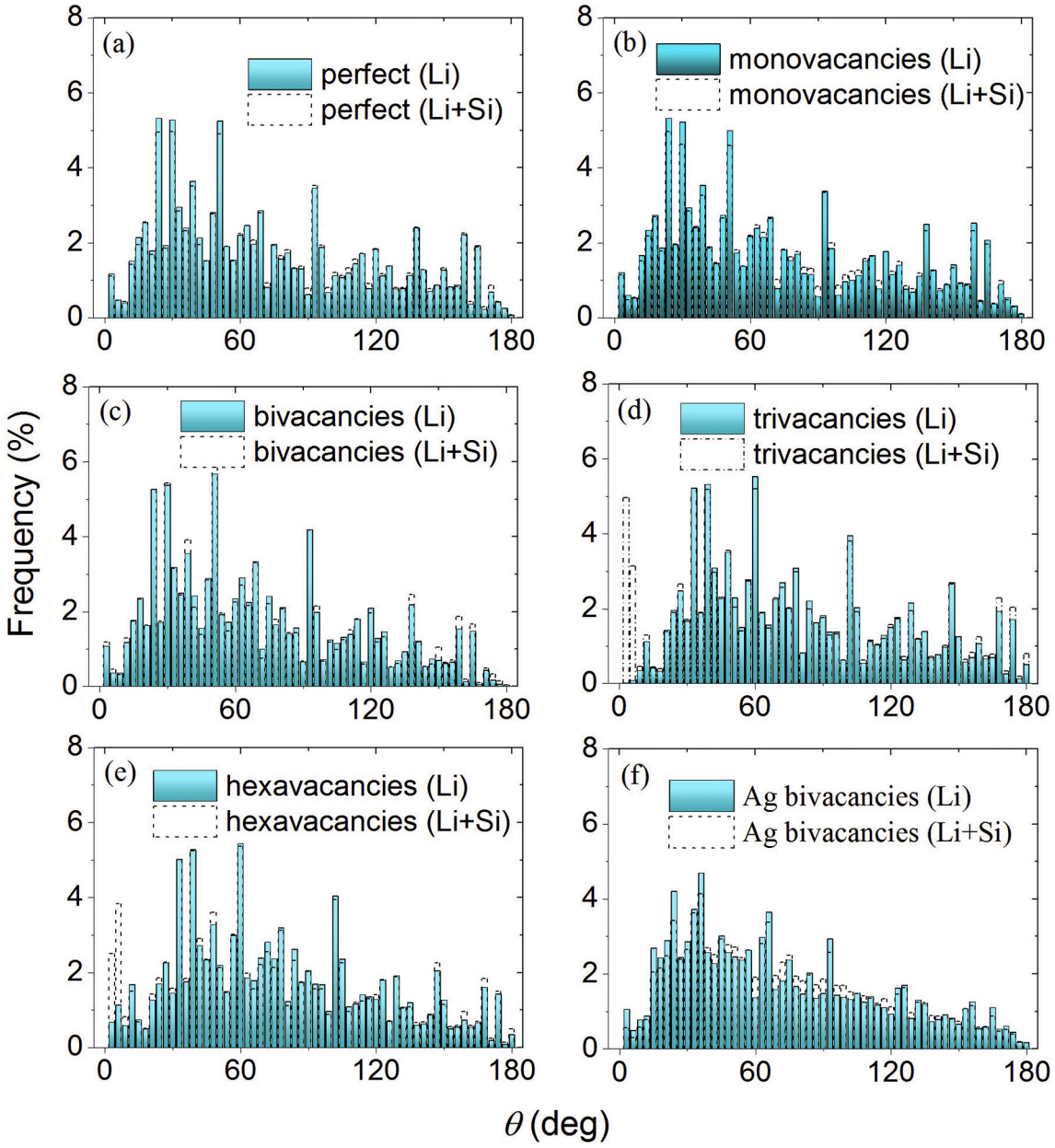

Fig. 7. The angular distribution of the nearest neighbors for lithium atoms after instant when the silicene channel is completely filled: (a)–(e) on a Ni(111) substrate, (f) on an Ag(111) substrate. Solid (colored) histograms are obtained when only Li atoms represent neighbors; dotted histograms correspond to the case when neighbors are selected from both Li atoms and Si atoms. The types of defects in silicene and the neighbors under consideration (in parentheses) are indicated in the captions in the margins of figures (a)–(f).

large defects – trivacancies. The shape of these defects is somewhat better preserved in the top sheet. In the bottom sheet, some trivacancies have adjacent smaller defects. Such defects are five-link, seven-link and eight-link rings. The size of the last defect is close to half the average size of the tri-vacancy in this sheet. There is an uneven “deposition” of lithium atoms on the upper and lower sheets of silicene.

Separated by a conditional horizontal plane passing through the midpoint of the initial gap, the lithium atoms were distributed as follows: 37 Li were based near the top sheet and only 23 - near the bottom sheet. We notice that a significant part of Li atoms is located above the centers of the hexagonal rings formed by the Si atoms of both the upper and lower sheets. Near each sheet there are also local clusters of Li atoms. There is a significant irregularity in the distribution of lithium atoms over the area of silicene sheets.

3.3. Detailed structure of lithium in the channel

The angular distributions (θ spectra) of the nearest neighbors for Li atoms that filled the silicene channel on the Ni(111) substrate contain characteristic peaks (Fig. 7) related to angles of 30°, 60°, 90°, 120° and 150°, which indicates the location of a part of Li atoms over the centers of hexagonal cells in silicene (Fig. 7). The sharp peaks in the θ spectrum of silicene with bivacancies on the Ni(111) substrate are more clearly pronounced than the corresponding peaks in the same type of silicene on an Ag(111) substrate. This indicates a larger number of Li atoms adsorbed on the centers of hexagonal Si cells in the first case, as compared with the second. When neighbors are selected from both Li atoms and Si atoms, only the θ distributions for silicene with three- and hexvacancies contain a pronounced small-angle peak (with $\theta \leq 6°$). In all other cases, this peak is weak enough.

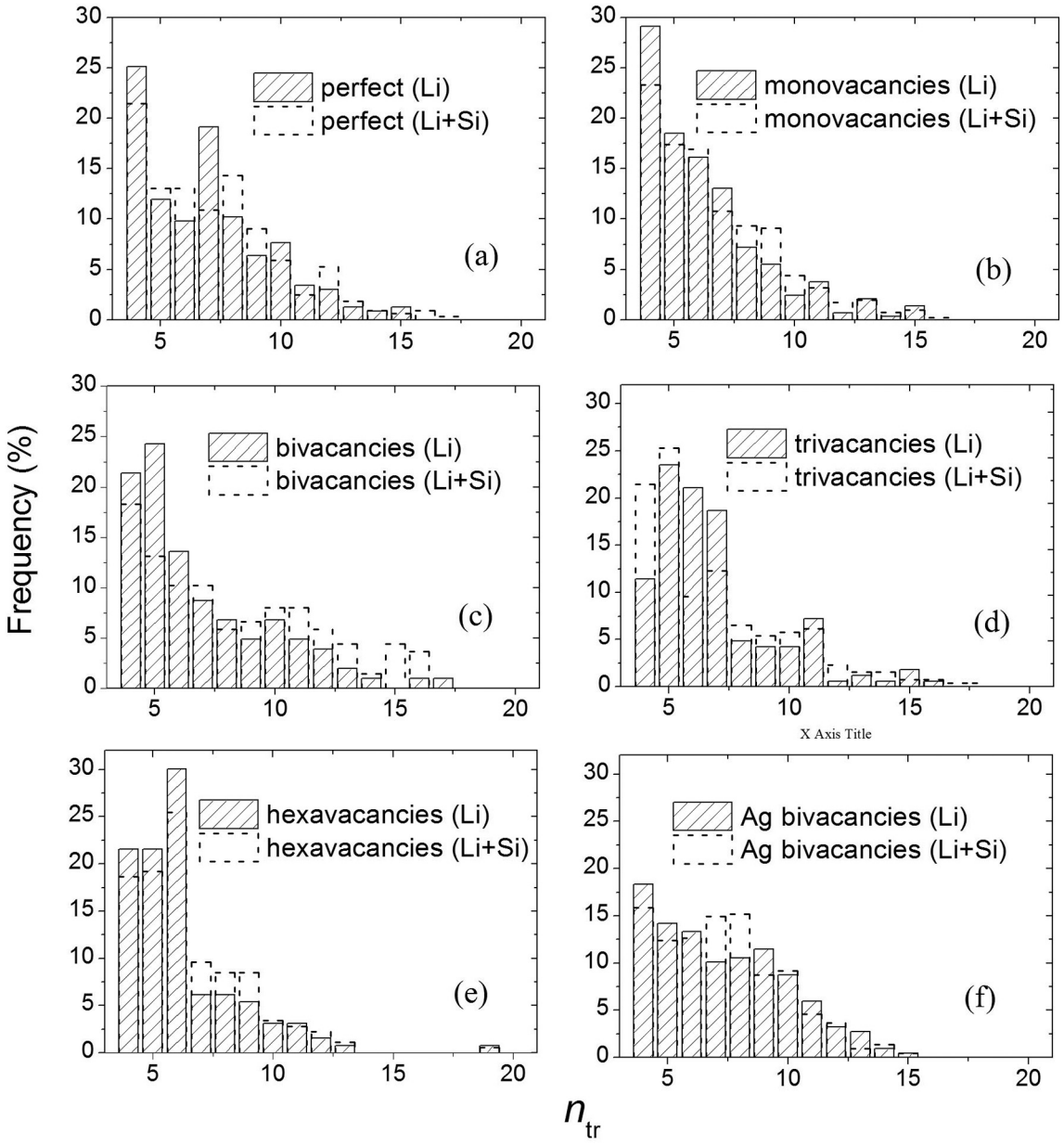

Fig. 8. The distributions of simplified polyhedra and combined simplified polyhedra with respect to the number of faces (n). SPs and CSPs are built for lithium atoms after the complete filling of a silicene channel, which is located: (a)–(e) on a Ni(111) substrate, (f) on an Ag(111) substrate. Solid (colored) histograms present the case when only Li atoms represent neighbors; dotted histograms give an idea of the local packing of atoms when neighbors are selected from both Li atoms and Si atoms. The types of defects in silicene and considered neighbors (in parentheses) are indicated in the captions in the margins of figures (a)–(f).

The distribution of simplified polyhedra by the number of faces in each of the cases considered here extends to values $n \leq 17$ (Fig. 8). Boundary conditions, i.e. the type of walls of the silicene channel, leave their mark on these distributions. If the channel walls are formed from perfect silicon or silicon with monovacancies, then the maximum values of the n spectrum fall on $n = 4$. However, with an increase in the size of defects, the maximum of the n spectrum begins to shift towards larger values of n. So, in the presence of bi-and tri-vacancies, the maximum of the n spectrum shifts to $n = 5$, and in the case of hexavacancies, its location is defined as $n = 6$. In addition, the intensity of of the n spectrum at $n = 4$ for a channel with trivacancies is almost two times lower than for the channel with bivacancies. The shape of the n spectrum for simplified polyhedral is also sensitive to the substrate material. So if there are bivacancies in the channel walls for a channel on an Ag (111) substrate, the maximum of the n spectrum falls on $n = 4$, while for a channel on a Ni(111) substrate it is located at $n = 5$. In addition, in this case the n spectrum for a channel on an Ag(111) substrate has a more uniform distribution of faces according to the number of sides contained in them. When the defects in the channel walls on the Ni (111) substrate become large (that is, when there are three and hexavacancies), the n spectrum is divided into two parts, which differ greatly in intensity.

Thus, the n spectrum of simplified polyhedra shows a high sensitivity both to the type of defects in the channel walls and to the substrate material on which this channel is located. The distribution of SP faces by the number of sides almost does not change its appearance when the size of defects in the walls of the silicene channel is changed. Statistical analysis of VP and their faces does not give obvious structural differences between the packings of lithium in the channels, which differ in both the walls and the substrate on which they are located. Corresponding distributions are presented in supplementary materials.

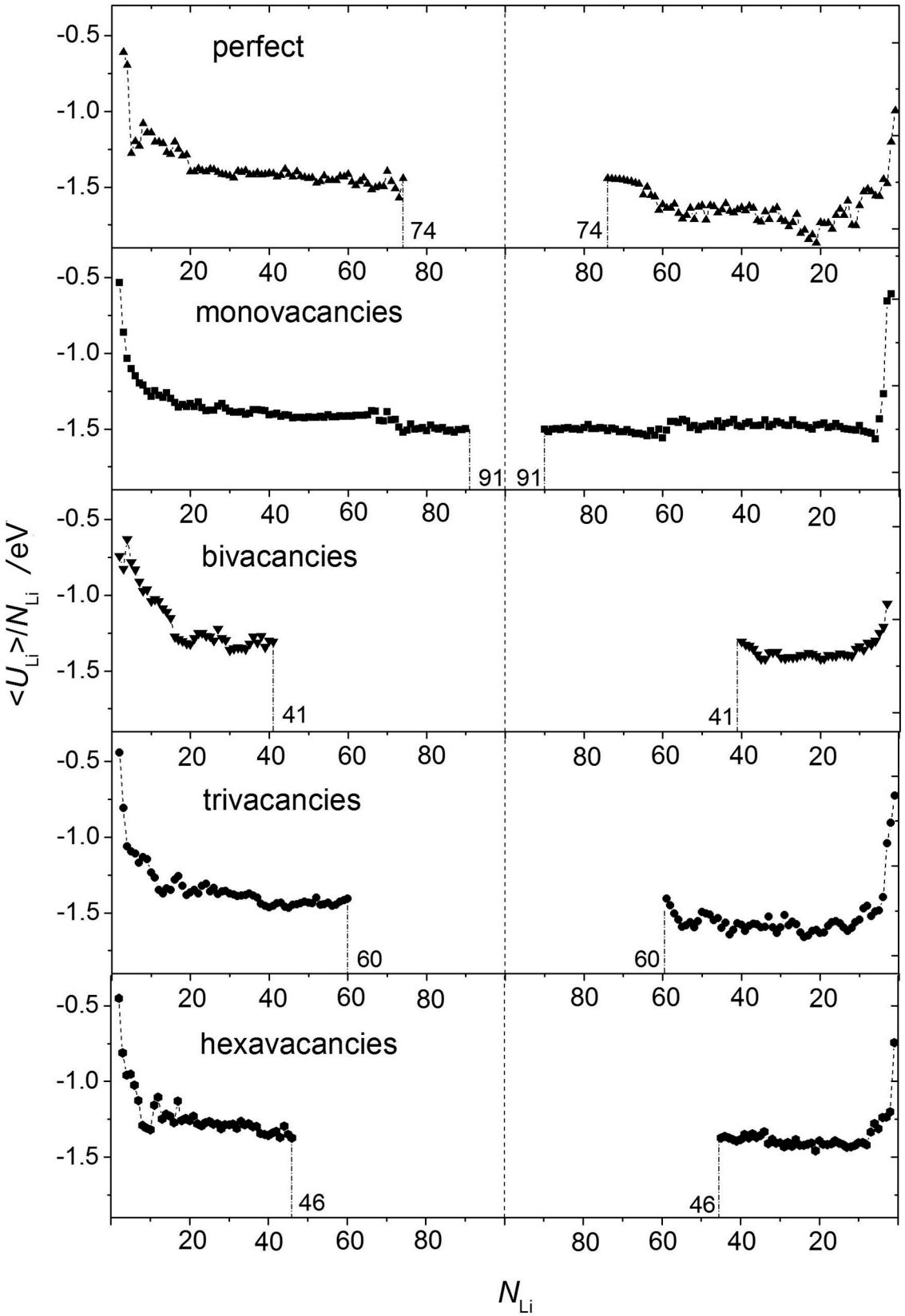

Fig. 9. Internal energy of lithium atoms at lithiation (left) and delithiation (right) in various flat silicene channels. N_{Li} is the number of lithium atoms in the channel. The maximum achievable number of lithium atoms in the channel is marked with a dash-dotted line.

3.4. System energy and stress distribution in silicene

The behavior of the specific internal energy $\langle U_{Li}/N_{Li}\rangle$ of Li atoms during lithiation and delithiation is reflected in Fig. 9. After the first 10–18 Li^+ ions enter the channel, a rapid decrease in energy $\langle U_{Li}/N_{Li}\rangle$ is observed, which is caused by the presence of ions (atoms) in

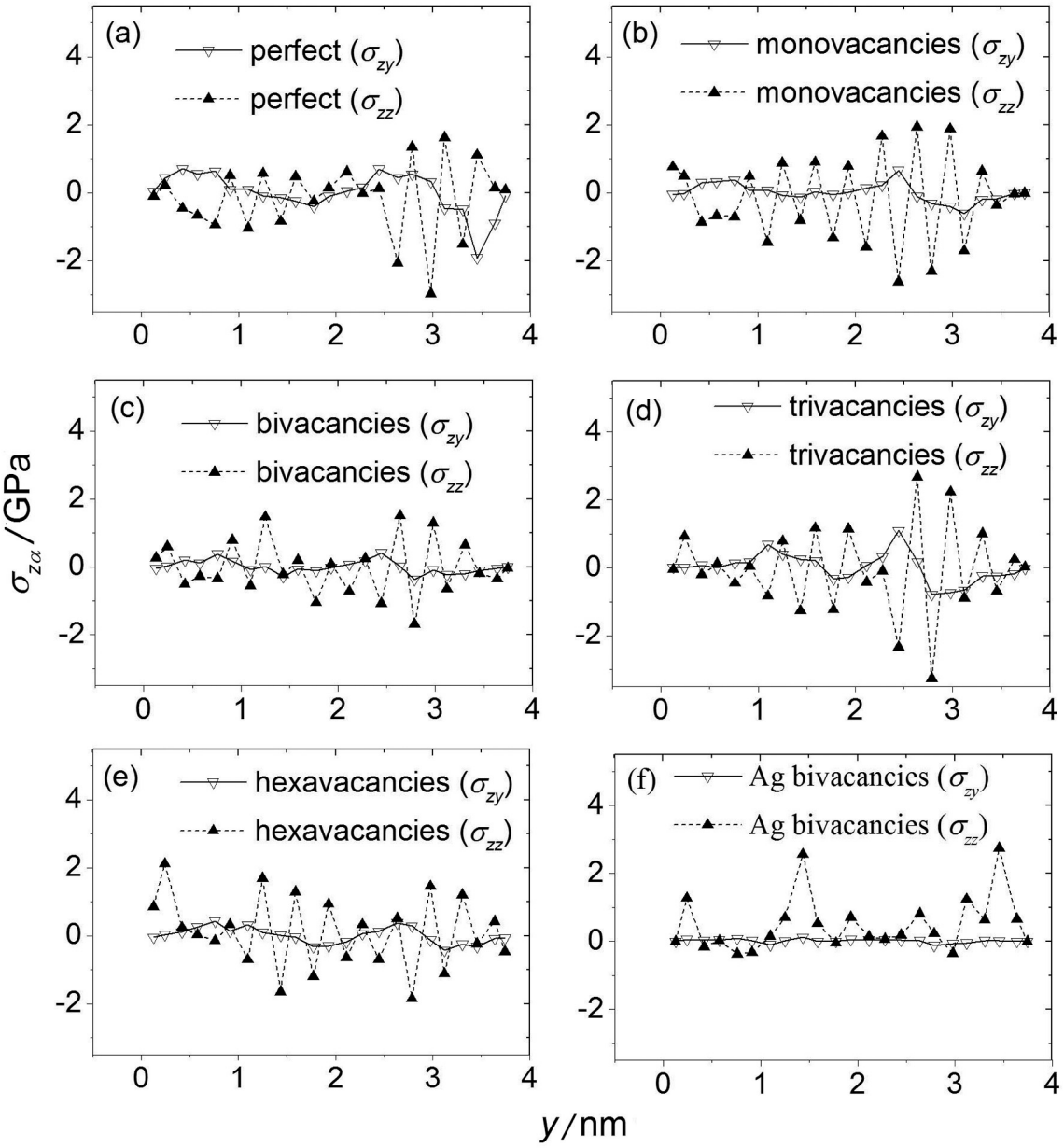

Fig. 10. The distribution of the average σ_{zx} and σ_{zz} stresses in the sheets of silicene along the 0*y* (armchair) direction when lithium fills the silicene channel located on a Ni(111) substrate. Elementary platforms are elongated along the axis 0*x*. The types of defects in silicene and the stresses in question (in parentheses) are indicated in the captions in the margins of figures (a)–(f).

energetically favorable places in the channel. With further increase of Li atoms in the channel due to their binding to Si atoms of the upper and lower sheets of silicene, rapid decrease is replaced by a slow decrease in energy $\langle U_{Li}/N_{Li}\rangle$. Lithium ions (atoms) have the ability to bind with defects. Ultimately, the energy $\langle U_{Li}/N_{Li}\rangle$ stabilizes in a neighborhood of a certain level.

The initial stage of delithiation is accompanied by small energy fluctuations. These fluctuations are associated with structural rearrangements caused by the exit of one of the ions from the channel. Up to a certain point, this process continues with decreasing energy $\langle U_{Li}/N_{Li}\rangle$. However, when a channel contains from 4 to 6 Li atoms, the energy $\langle U_{Li}/N_{Li}\rangle$ may increase greatly due to the acquisition by the Li^+ ion, and then the Li atoms, of high kinetic energy values. This phenomenon applies to all the cases considered here, regardless of whether there are defects in the channel walls. The internal energy of Li atoms behaves in many ways identical when the channels are filled with lithium on Ni (111) and Ag (111) substrates. Thus, this characteristic is not very sensitive to the type of substrate.

The most significant local stresses when division sheets of silicene along the 0*y* axis are higher than in the case when the elementary areas are elongated along the 0*x* axis. The distribution of stresses averaged over both silicene sheets (located on the Ni(111) surface), when an observation is carried out along the 0*y* direction, is shown in Fig. 10. In this case, the stresses σ_{zz} turn out to be higher than the stresses σ_{zy}. Stronger σ_{zz} stresses arise when lithium is introduced into a perfect silicene channel or a channel with walls that have mono- and trivacancies. These stresses are commensurate with the stresses σ_{zz} arising due to the filling the channel with lithium when the channel walls have monovacancies, and the channel is located on an Ag(111) substrate. However, the maximum values of local stresses are no more than 25% of the tensile strength (12.5 GPa) of a silicene sheet [50]. Thus, when the silicon channel is completely filled with lithium, the stresses arising in its walls are not critical to the loss of the mechanical strength of silicene.

4. Conclusion

The results obtained in this article indicate that nickel is a very good substrate material for silicon, when this combination is used as an anode LIB. Based on a numerical experiment, we have established that the mechanical characteristics of a silicene-nickel anode meet the necessary requirements for its use in LIB. The profile of the packing density of Li atoms in a perfect silicene channel and in channels with walls having vacancy-type defects showed a high intensity of filling with lithium at the middle level in the channel gap. This feature is caused by the influence of the Ni(111) substrate, since similar channels on an Ag(111) substrate have a different type of lithium filling, so that the majority of Li atoms concentrate near the channel walls. It should be noted that the Ni(111) substrate exerts a stabilizing effect on the structure of the defective silicene forming the channel walls when the channel is filled with lithium. Even trivacancies in both sheets of silicene mostly retain their shape and size. In silicene channels on metal (Ag, Al, Cu) substrates, vacancy defects have largely changed their shape and size. They can disappear or form the larger pores with a jagged border as well as turn into rounded pores under the influence of lithium introduced into the channel.

It has been established that the use of silicene containing monovacancies can significantly increase the occupancy of the channel with lithium. Consequently, the use of such a silicene as an anode material will markedly increase the capacity of the electrode. Moreover, during cycling there will be no stress in it, which can lead to the destruction of the anode. Nickel substrate is not in direct contact with the electrolyte. Therefore, the metal has a low likelihood of corrosion.

Thus, nickel remains a promising candidate as a substrate material for silicene, oriented on the use in a new generation of electrochemical devices.

Declaration of Competing Interest

The author declares that he has no known competing financial interests or personal relationships that could have appeared to influence the work reported in this paper.

Acknowledgements

This work is sponsored by the Ministry of Education and Science of the Russian Federation and is performed in the frame of the State Assignment number 075-03-2020-582/1 dated 18.02.2020 (the topic number 0836-2020-0037).

Appendix A. Supplementary data

Supplementary data to this article can be found online at https://doi.org/10.1016/j.ssi.2020.115463.

References

[1] F. Wu, J. Maier, Y. Yu, Guidelines and trends for next-generation rechargeable lithium and lithium-ion batteries, Chem. Soc. Rev. 49 (2020) 1569–1614, https://doi.org/10.1039/C7CS00863E.
[2] Y. Jin, B. Zhu, Z. Lu, N. Liu, J. Zhu, Challenges and recent progress in the development of Si anodes for lithium-ion battery, Adv. Energy Mater. 7 (2017) 1700715, , https://doi.org/10.1002/aenm.201700715.
[3] C.K. Chan, H. Peng, G. Liu, K.M. Wrath, X.F. Zhang, R.A. Huggins, Y. Cui, High-performance lithium battery anodes using silicon nanowires, Nat. Nanotechnol. 3 (2008) 31–35, https://doi.org/10.1038/nnano.2007.411.
[4] S. Hao, B. Ouyang, C. Li, B. Zhang, J. Feng, J. Wu, Hollow mesoporous $Co(PO_3)_2$ - carbon polyhedra as high performance anode materials for lithium ion batteries, J. Phys. Chem. C 123 (14) (2019) 8599–8606, https://doi.org/10.1021/acs.jpcc.8b12494.
[5] A.E. Galashev, O.R. Rakhmanova, Yu.P. Zaikov, Defect silicene and graphene as applied to the anode of lithium-ion batteries: numerical experiment, Phys. Solid State 58 (2016) 1850–1857, https://doi.org/10.1134/S1063783416090146.
[6] Z. Ni, H. Zhong, X. Jiang, R. Quhe, Y. Wang, J.-J. Shi, J. Lu, Nanoscale 6 (2014) 7609–7618, https://doi.org/10.1039/c4nr00028e.
[7] V.B. Shenoy, P. Johari, Y. Qi, Elastic softening of amorphous and crystalline Li–Si phases with increasing Li concentration: a first-principles study, J. Power Sources 195 (2010) 6825–6830, https://doi.org/10.1016/j.jpowsour.2010.04.044.
[8] K. Zhao, W.L. Wang, J. Gregoire, M. Pharr, Z. Suo, J.J. Vlassak, E. Kaxiras, Lithium-assisted plastic deformation of silicon electrodes in lithium-ion batteries: a first-principles theoretical study, Nano Lett. 11 (2011) 2962–2967, https://doi.org/10.1021/nl201501s.
[9] V.A. Sethuraman, M.J. Chon, M. Shimshak, V. Srinivasan, P.R. Guduru, In situ measurements of stress evolution in silicon thin films during electrochemical lithiation and delithiation, J. Power Sources 195 (2010) 5062–5066, https://doi.org/10.1016/j.jpowsour.2010.02.013.
[10] M. Pharr, Z. Suo, J.J. Vlassak, Measurements of the fracture energy of lithiated silicon electrodes of Li-ion batteries, Nano Lett. 13 (2013) 5570–5577, https://doi.org/10.1021/nl403197m.
[11] A.Y. Galashev, K.A. Ivanichkina, Computer study of atomic mechanisms of intercalation/deintercalation of Li ions in a silicene anode on an Ag (111) substrate, J. Electrochem. Soc. 165 (2018) 1788–1796, https://doi.org/10.1149/2.0751809JES.
[12] A.Y. Galashev, K.A. Ivanichkina, Computer test of a new silicene anode for lithium-ion battery, ChemElectroChem. 6 (2019) 1525–1535, https://doi.org/10.1002/celc.201900119.
[13] A.Y. Galashev, K.A. Ivanichkina, Computational investigation of a promising Si-Cu anode material, Phys. Chem. Chem. Phys. 21 (2019) 12310–12320, https://doi.org/10.1039/C9CP01571J.
[14] A.Y. Galashev, K.A. Ivanichkina, K.P. Katin, M.M. Maslov, Computer test of a modified silicene/graphite anode for lithium-ion batteries, ACS Omega (2020), https://doi.org/10.1021/acsomega.0c01240.
[15] A.Y. Galashev, K.A. Ivanichkina, Silicene anodes for lithium-ion batteries on metal substrates, J. Electrochem. Soc. 167 (2020) 050510, , https://doi.org/10.1149/1945-7111/ab717a.
[16] A.Y. Galashev, A.S. Vorob'ev, Physical properties of silicene electrodes for Li-, Na-, Mg-, and K-ion batteries, J. Solid State Electrochem. 22 (2018) 3383–3391, https://doi.org/10.1007/s10008-018-4050-8.
[17] S.S. Talebi, K. Irai, J. Beheshtian, Theoretical prediction of silicene; as new candidate for the anode of lithium-ion batteries, Phys. Chem. Chem. Phys. 17 (44) (2015) 29689–29696, https://doi.org/10.1039/c5cp04666a.
[18] M. Yao, L. Ai, Y. Zhou, J. Ma, M. Chen, Structural damage of few-layer silicene in vertical and parallel lithiations, J. Electrochem. Soc. 166 (2019) A3394–A3400, https://doi.org/10.1149/2.1051914jes.
[19] S. Li, Y. Wu, Y. Tu, Y. Wang, T. Jiang, W. Liu, Y. Zhao, Defects in silicene: vacancy clusters, extended line defects, and di-adatoms, Sci. Rep. 5 (2014) 7881, https://doi.org/10.1038/srep07881.
[20] G. Brumfiel, Sticky problem snares wonder material, Nature 495 (2013) 152–153 http://li.mit.edu/S/2d/Paper/Brumfiel13.pdf.
[21] J.F. Guo, J.F. Zhang, H.S. Liu, Q.F. Zhang, J.J. Zhao, Structures, mobilities, electronic and magnetic properties of point defects in silicone, Nanoscale 5 (2013) 9785–9792, https://doi.org/10.1039/c3nr02826g.
[22] J.K. Lee, J.-H. Shin, H. Lee, W.Y. Yoon, Characterization of nano silicon on nano-pillar-patterned nickel substrate for lithium ion batteries, J. Electrochem. Soc. 161 (2014) A1480–A1485, https://doi.org/10.1149/2.0131410jes.
[23] G. Ferraresi, L. Czornomaz, C. Villevieille, P. Novák, M. El Kazzi, Elucidating the surface reactions of an amorphous Si thin film as a model electrode for Li-ion batteries, ACS Appl. Mater. Interfaces (2016) 29791–29798, https://doi.org/10.1021/acsami.6b10929 8, 43.
[24] A.E. Galashev, K.A. Ivanichkina, A.S. Vorobev, O.R. Rakhmanova, Structure and stability of defective silicene on Ag(001) and Ag(111) substrates: a computer experiment, Phys. Solid State 59 (6) (2017) 1242–1252, https://doi.org/10.1134/S1063783417060087.
[25] A.Y. Galashev, K.A. Ivanichkina, Nanoscale simulation of the lithium ion interaction with defective silicene, Phys. Lett. A 381 (2017) 3079–3083, https://doi.org/10.1016/j.physleta.2017.07.040.
[26] A.Y. Galashev, K.A. Ivanichkina, O.R. Rakhmanova, Yu.P. Zaikov, Physical aspects of the lithium ion interaction with the imperfect silicene located on a silver substrate, Lett. Mater. 8 (2018) 463–467, https://doi.org/10.22226/2410-3535-2018-4-463-467.
[27] G. Ferraresi, M. El Kazzi, L. Czornomaz, C.-L. Tsai, S. Uhlenbruck, C. Villevieille, Electrochemical performance of all-solid-state Li-ion batteries based on garnet electrolyte using silicon as a model electrode, ACS Energy Lett. 3 (2018) 1006–1012, https://doi.org/10.1021/acsenergylett.8b00264.
[28] J. Tersoff, Modeling solid-state chemistry: interatomic potentials for multicomponent systems, Phys. Rev. B Condens. Matter 39 (1989) 5566–5568, https://doi.org/10.1103/PhysRevB.39.5566.
[29] Y. Mishin, D. Farkas, M.J. Mehl, D.A. Papaconstantopoulos, Interatomic potentials for monoatomic metals from experimental data and ab initio calculations, Phys. Rev. B 59 (5) (1999) 3393–3407, https://doi.org/10.1103/physrevb.59.3393.
[30] R. Yu, P. Zhai, G. Li, L. Liu, Molecular dynamics simulation of the mechanical properties of single-crystal bulk Mg_2Si, J. Electron. Mater. 41 (2012) 1465–1469, https://doi.org/10.1007/s11664-012-1916-x.
[31] E.C. Angel, J.S. Reparaz, J. Gomis-Bresco, M.R. Wagner, J. Cuffe, B. Graczykowski, A. Shchepetov, H. Jiang, M. Prunnila, J. Ahopelto, F. Alzina, C.M. Sotomayor Torres, Reduction of the thermal conductivity in free-standing silicon nano-membranes investigated by non-invasive Raman thermometry, APL Mater. 2 (2014) 012113, , https://doi.org/10.1063/1.4861796.
[32] S.K. Das, D. Roy, S. Sengupta, Volume change in some substitutional alloys using Morse potential function, J. Phys. F: Met. Phys. 7 (1977) 5–14 http://iopscience.iop.org/0305-4608/7/1/011.

[33] K. Muller, F.F. Krause, A. Beche, M. Schowalter, V. Galioit, S. Loffler, J. Verbeeck, J. Zweck, P. Schattschneider, A. Rosenauer, Atomic electric fields revealed by a quantum mechanical approach to electron picodiffraction, Nat. Commun. 5 (2014) 5653, https://doi.org/10.1038/ncomms6653.
[34] K. Kawahara, T. Shirasawa, R. Arafune, C.-L. Lin, T. Takahashi, M. Kawai, N. Takagi, Determination of atomic positions in silicene on Ag(111) by low-energy electron diffraction, Surf. Sci. 623 (2014) 25–28, https://doi.org/10.1016/j.susc.2013.12.013.
[35] Y. Du, J. Zhuang, J. Wang, Z. Li, H. Liu, J. Zhao, X. Xu, H. Feng, L. Chen, K. Wu, X. Wang, S.X. Dou, Quasi-freestanding epitaxial silicene on Ag(111) by oxygen intercalation, Sci. Adv. 2 (2016) e1600067, , https://doi.org/10.1126/sciadv.1600067.
[36] H. Liu, H. Feng, Y. Du, J. Chen, K. Wu, J. Zhao, Point defects in epitaxial silicene on Ag(111) surfaces, 2D Materials 3 (2016) 025034, , https://doi.org/10.1088/2053-1583/3/2/025034.
[37] A.E. Galashev, Yu.P. Zaikov, R.G. Vladykin, Effect of electric field on lithium ion in silicene channel. Computer experiment, Russ. J. Electrochem. 52 (2016) 966–974, https://doi.org/10.1134/S1023193516100049.
[38] A.J. Pearse, T.E. Schmitt, E.J. Fuller, F. El-Gabaly, C.-F. Lin, K. Gerasopoulos, A.C. Kozen, A.A. Talin, G. Rubloff, K.E. Gregorczyk, Nanoscale solid state batteries enabled by thermal atomic layer deposition of a lithium polyphosphazene solid state electrolyte, Chem. Mater. 29 (8) (2017) 3740, https://doi.org/10.1021/acs.chemmater.7b00805.
[39] A.E. Galashev, Yu.P. Zaikov, Computer simulation of Li^+ ion interaction with a graphene sheet, Rus. J. Phys. Chem. A 89 (2015) 2243–2247, https://doi.org/10.1134/S0036024415120122.
[40] E. Hüger, H. Schmidt, Lithium permeability increase in nanosized amorphous silicon layers, J. Phys. Chem. C 122 (50) (2018) 28528–28536, https://doi.org/10.1021/acs.jpcc.8b09719.
[41] T.H. Osborn, A.A. Farajian, Stability of lithiated silicene from first principles, J. Phys. Chem. C 116 (2012) 22916–22920, https://doi.org/10.1021/jp306889x.
[42] A.K. Subramaniyan, C.T. Sun, Continuum interpretation of virial stress in molecular simulations, Int. J. Solids Struct. 45 (2008) 4340–4346, https://doi.org/10.1016/j.ijsolstr.2008.03.016.
[43] A.Y. Galashev, Computer study of the removal of Cu from the graphene surface using Ar clusters, Comput. Mater. Sci. 98 (2015) 123–128, https://doi.org/10.1016/j.commatsci.2014.11.002.
[44] A.Y. Galashev, K.A. Ivanichkina, Computational study of the properties of silicon thin films on graphite, Rus. J. Phys. Chem. A 91 (12) (2017) 2448–2452, https://doi.org/10.1134/S003602441712007X.
[45] O.A. Novruzova, O.R. Rakhmanova, A.E. Galashev, The stability and structure of $(N_2)_j(H_2O)_i$ and $(Ar)_j(H_2O)_i$ clusters, Rus. J. Phys. Chem. A 81 (2007) 1825–1828, https://doi.org/10.1134/S0036024407110180.
[46] A.Y. Galashev, Atomistic simulations of methane interactions with an atmospheric moisture, J. Chem. Phys. 139 (2013) 124303, https://doi.org/10.1063/1.4821192.
[47] S. Plimpton, Fast parallel algorithms for short-range molecular dynamics, J. Comput. Phys. 117 (1995) 1–19, https://doi.org/10.1006/jcph.1995.1039.
[48] T. Ichikawa, The assembly of hard spheres as a structure model of amorphous iron, Phys. Status Solidi (A) 29 (1) (1975) 293–302, https://doi.org/10.1002/pssa.2210290132.
[49] T.K. Min, T.L. Yoon, T.L. Lim, Molecular dynamics simulation of melting of silicene, Mater. Res. Express 5 (6) (2018) 065054, , https://doi.org/10.1088/2053-1591/aacdb7.
[50] Q.-X. Pei, Z.-D. Sha, Y.-Y. Zhang, Y.-W. Zhang, Effects of temperature and strain rate on the mechanical properties of silicone, J. Appl. Phys. 115 (2014) 023519, , https://doi.org/10.1063/1.4861736.